DALTON

Synthesis of complexes of dimethyltin(IV) with mono- and di-deprotonated pyridoxine (PN) in media with various anions. Crystal structures of $[SnMe_2(PN - H)]NO_3 \cdot 2H_2O$, $[SnMe_2(H_2O)(PN - H)]Cl \cdot H_2O$ and $[SnMe_2(H_2O)(PN - 2H)] \cdot 0.5H_2O$

José S. Casas,[a] Eduardo E. Castellano,[b] Félix Condori,[a] María D. Couce,[c] Agustín Sánchez,[a] José Sordo,*[,a] José Mª Varela[a] and Julio Zuckerman-Schpector[b]

[a] *Departamento de Química Inorgánica, Universidade de Santiago de Compostela, 15706 Santiago de Compostela, Galicia, Spain*
[b] *Instituto de Fisica e Química de São Carlos, Universidade de São Paulo, São Carlos, SP, Brazil*
[c] *Departamento de Química Inorgánica, Universidade de Vigo, Galicia, Spain*

The reaction of the dimethyltin(IV) cation with pyridoxine [3-hydroxy-4,5-bis(hydroxymethyl)-2-methylpyridine, PN] has been investigated in ethanol–water (80 : 20 v/v) containing NO_3^- and Cl^-, NO_3^- and $MeCO_2^-$ or Cl^- and $MeCO_2^-$ ions in various mole ratios. The compounds $[SnMe_2(PN - H)]NO_3 \cdot 2H_2O$ **1**, $[SnMe_2(H_2O)(PN - H)]Cl \cdot H_2O$ **2** and $[SnMe_2(H_2O)(PN - 2H)] \cdot 0.5H_2O$ **3** were isolated and characterized by IR, Raman, cross polarization magic angle spinning ^{13}C NMR and electron impact and FAB mass spectrometry. The structures of the compounds were determined by X-ray diffraction. In **1** $[SnMe_2(PN - H)]_2^{2+}$ units in which each mono-deprotonated pyridoxine co-ordinates to one tin atom *via* the phenolic O and a deprotonated CH_2OH group O and to the other *via* the latter group alone are connected in a polymeric structure *via* the other CH_2OH group of each PN − H. In each dimeric unit the tin atom is co-ordinated to two methyl groups, the phenolic O atom, the O atoms of two deprotonated CH_2OH groups, and the O atom of a non-deprotonated CH_2OH group. Hydrogen-bonded water and NO_3^- ions are also present in the crystal lattice. In **2** the lattice contains dimeric $[SnMe_2(H_2O)(PN - H)]_2^{2+}$ units (in which the tin–pyridoxine co-ordination is the same as in **1** except that the bonds connecting different units in **1** now bind aqua ligands) and hydrogen-bonded water and chloride ions. In **3** the crystal contains dimeric $[SnMe_2(H_2O)(PN - 2H)]_2$ units (in which the dideprotonated ligand co-ordinates as in **2**) and water. The behaviour of these compounds in D_2O and $(CD_3)_2SO$ was studied by NMR spectroscopy.

The wide use of organotin(IV) compounds has increased interest in their environmental and biological chemistry.[1] In particular, considerable attention has been given to the thermodynamics of the hydrolysis equilibria of diorganotin cations[2] and of their co-ordination to other ligands in aqueous solution.[3] Most such studies have been carried out in media with a single counter ion and at a single value of ionic strength, but recent research[4] has investigated the behaviour of organotin compounds in a multicomponent solution closer in composition to natural fluids. This approach is particularly valuable as regards the effects of the chloride ion, which has appreciable capacity to co-ordinate to organometallic cations and is present in significant concentrations in extracellular body fluids and environmental waters (especially sea-water). In the first of an ongoing series of studies of the interaction of diorganotin compounds with vitamins in aqueous or aqueous–organic media[5] we recently isolated[5b] a thiaminium dimethyltin(IV) complex and a thiaminium diphenyltin(IV) complex with different degrees of involvement of chloride ions [thiaminium = 3-(4-amino-2-methylpyrimidin-5-ylmethyl)-5-(2-hydroxyethyl)-4-methylthiazolium]. In continuation of this work, the ultimate aims of which are to contribute to understanding of the biological activity of organotin(IV) cations and to discover biological ligands capable of modifying this activity,[6] we have now investigated the interaction, in the presence of various anions, between the dimethyltin(IV) cation and pyridoxine [3-hydroxy-4,5-bis(hydroxymethyl)-2-methylpyridine] (PN), one of the recognized forms of vitamin B_6.[7]

The protonation equilibria of pyridoxine can be described as in Scheme 1. All these forms possess a number of potential co-ordination sites, especially the neutral species **Ia** and **Ib** and the anionic species **II**, but the set of sites varies from one species to another. Hence controlling the relative concentrations of the various pyridoxine species by using different solvents (PN exists in the zwitterionic form **Ib** in aqueous solution, but as **Ia** in

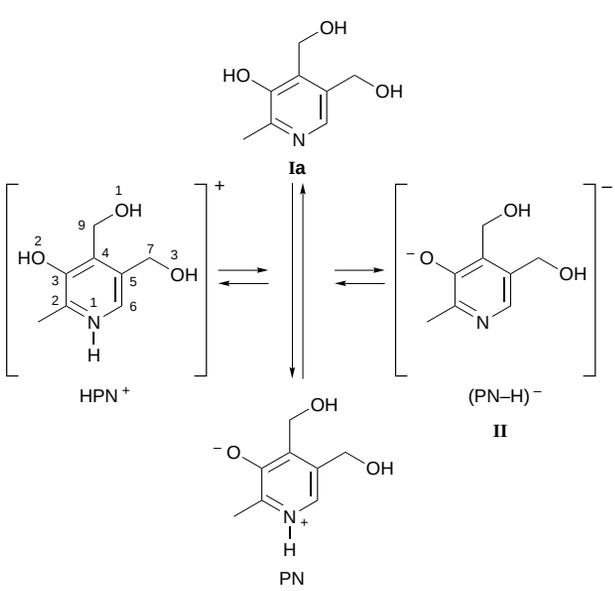

Scheme 1

1,4-dioxane and alcohols) should allow the preparation of complexes in which pyridoxine co-ordinates *via* different donor sites.[8]

Complexes of the different forms of pyridoxine with transition elements have been structurally characterized by X-ray diffraction[8,9] and those in the neutral form with rare-earth elements have also been prepared.[10] By contrast, relatively little is known of the interaction of this compound with typical main-group elements.[11,12] The only structure determined is that of $[Cd(PN)Cl_2]$.[11a] In the case of tin,[12] $[SnMe_2(PN - 2H)]$ and $[SnBu_2(PN - 2H)]$ have been prepared by treating the corresponding dialkyltin oxide with pyridoxine in a non-aqueous medium, and found to have high activity against certain tumour cell lines, but no structural data are available.

This paper describes the interaction of pyridoxine with dimethyltin(IV) in the presence of the nitrate, acetate and chloride anions in ethanol–water (80:20 v/v) and reports the crystal structures of $[SnMe_2(PN - H)]NO_3\cdot 2H_2O$ **1**, $[SnMe_2(H_2O)(PN - H)]Cl\cdot H_2O$ **2** and $[SnMe_2(H_2O)(PN - 2H)]\cdot 0.5H_2O$ **3**. The pyridoxine ligand exhibits three different co-ordination modes in these three compounds: in **1** it is monodeprotonated and its co-ordination to three different Sn atoms [one of them chelated by O(1) and O(2)] involves all three O atoms [including the protonated O(3)]; in **2** it is monodeprotonated as in **1** but no longer co-ordinates *via* O(3); and in **3** it co-ordinates in the same way as in **2** but is dideprotonated. As far as we know, the co-ordination mode present in **1** has not hitherto been observed in monodeprotonated pyridoxine complexes, and the dideprotonated pyridoxine ligand present in **3** has not previously been characterized structurally.

Experimental

Material and methods

Pyridoxine hydrochloride (Aldrich), dimethyltin dichloride (Aldrich), silver nitrate (Merck) and silver acetate (Probus) were used as received. Elemental analysis was performed with a Carlo Erba 1108 microanalyser. Melting points were determined with a Büchi apparatus. Mass spectra were recorded on a Kratos MS50TC spectrometer connected to a DS90 system and operating under electron impact (EI) conditions (direct insertion probe, 70 eV, 250 °C) and FAB (*m*-nitrobenzyl alcohol, Xe, 8 eV; *ca.* 1.28×10^{-18} J); ions were identified by DS90 software and the normal values for the metallated peaks were calculated using the isotope ^{120}Sn. Infrared (KBr pellets or Nujol mulls) and Raman spectra (polycrystalline samples) were recorded on a Bruker IFS66V FT-IR spectrometer equipped with an FRA-106 Raman accessory and are reported in the synthesis section using the following abbreviations: v = very, s = strong, m = medium, w = weak, sh = shoulder, br = broad. Proton and ^{13}C NMR spectra in solution were recorded at room temperature on a Bruker AMX 300 spectrometer operating at 300.14 and 75.40 MHz, respectively, using 5 mm outside diameter tubes; chemical shifts are reported relative to $SiMe_4$. Solid-state NMR spectra were recorded on a Bruker AMX 300 spectrometer at 75.40 MHz using 7 mm outside diameter zirconia rotors and on a Bruker DSX 500 spectrometer at 125.77 MHz using 4 mm outside diameter zirconia rotors; chemical shifts are referred to glycine (δ 176.26). The conductivities of 10^{-3} M solutions were measured in a Crison MicroCM2202 conductivity meter.

Synthesis of the compounds

$[SnMe_2(PN - H)]NO_3\cdot 2H_2O$ 1. To PN·HCl (2.06 g, 10 mmol) dissolved in ethanol–water (80:20 v/v, 50 cm^3) were added solid NaOH (0.40 g, 10 mmol) and solid $AgNO_3$ (1.70 g, 10 mmol); the AgCl formed after stirring was filtered out to leave solution A. To $SnMe_2Cl_2$ (1.10 g, 5 mmol) in the same solvent (20 cm^3) was added solid $AgNO_3$ (1.70 g, 10 mmol) and the AgCl formed after stirring was filtered out to leave solution B. Solution B was added with stirring to A, and stirring was continued for 1 d. After 12 h of standing well formed crystals were observed; this first batch was filtered out 12 h later {Found: C, 28.9; N, 6.8; H, 4.9. Calc. for $[SnMe_2(PN - H)]NO_3\cdot 2H_2O$: C, 28.9; N, 6.7; H, 4.8%}. M.p. >300. Yield (first batch) 41%. Main metallated signals in the EI mass spectrum: at *m*/*z* 317 {$[SnMe_2(PN - H)]$, 62.5}, 299 {$[SnMe_2(PN - 2H - OH)]$, 100.0}, 285 {$[SnMe_2(PN - 2H - CH_2OH)]$, 47.6}, 240 {$[SnMe_2(PN + H - 2CH_2OH - OH)]$, 18.3}, 212 {$[SnMe_2(NO_3)]$, 81.9}, 167 {$[SnMe_2(OH)]$, 44.4}, 150 ($[SnMe_2]$, 19.6), 135 ([SnMe], 65.7) and 120 ([Sn], 31.1%). Besides these, the spectrum showed signals for pyridoxine and its fragments, and the FAB spectrum a signal at *m*/*z* 632 ($[\{SnMe_2(PN - 2H)\}_2]$, 5.3%). Infrared and Raman (in parentheses), cm^{-1}: 1630w (1633w, 1617w), 1530vs (1541w), 1474m (1471w), ν(ring); 995vs, ν(CO); 1383vs, $\nu_{asym}(NO_3^-)$; 1048m (1044m), $\nu_{sym}(NO_3^-)$; 575m (575m), ν_{asym}(Sn–C); 526m (525vs), ν_{sym}(Sn–C). Λ_M (dimethyl sulfoxide, dmso) 9.7 S cm^2 mol^{-1}.

$[SnMe_2(H_2O)(PN - H)]Cl\cdot H_2O$ 2. To PN·HCl (2.06 g, 10 mmol) dissolved in ethanol–water (80:20 v/v, 50 cm^3) was added solid NaOH (0.40 g, 10 mmol) (solution A). To $SnMe_2Cl_2$ (1.10 g, 5 mmol) in the same solvent (25 cm^3) was added solid $Ag(O_2CMe)$ (1.67 g, 10 mmol) and the AgCl formed after stirring was filtered out to leave solution B. Solution B was added with stirring to A, and stirring was continued for 1 d. After 12 h of standing well formed crystals were observed; this first batch was filtered out 12 h later {Found: C, 31.0; N, 3.5; H, 5.5. Calc. for $[SnMe_2(H_2O)(PN - H)]Cl\cdot H_2O$: C, 30.9; N, 3.6; H, 5.2%}. M.p. = 220 °C. Yield (first batch) 49%. Main metallated signals in the EI mass spectrum: *m*/*z* 150 ($[SnMe_2]$, 61.5), 135 ([SnMe], 11.9) and 120 ([Sn], 29.7%). Besides these the spectrum showed signals for pyridoxine and its fragments and the FAB spectrum signals at 632 ($[\{SnMe_2(PN - 2H)\}_2]$, 4.6), 318 ($[SnMe_2(PN)]$, 100), 299 {$[SnMe_2(PN - 2H - OH)]$, 8.8}, 285 {$[SnMe_2(PN - 2H - CH_2OH)]$, 20.3} and 240 {$[SnMe_2(PN + H - 2CH_2OH - OH)]$, 2.9%}. Infrared and Raman (in parentheses), cm^{-1}: 1640 (sh), δ(OH); 1624w (1622w, 1607w), 1527vs (1529w), 1462m (1460w), ν(ring); 1008vs, ν(CO); 583m (574w), ν_{asym}(Sn–C); 526 (sh), (520vs), ν_{sym}(Sn–C). Λ_M (dmso) 3.5 S cm^2 mol^{-1}.

$[SnMe_2(H_2O)(PN - 2H)]\cdot 0.5H_2O$ 3. To PN·HCl (2.06 g, 10 mmol) dissolved in ethanol–water (80:20 v/v, 50 cm^3) were added solid NaOH (0.40 g, 10 mmol) and $AgNO_3$ (1.70 g, 10 mmol); the AgCl formed after stirring was filtered out to leave solution A. To $SnMe_2Cl_2$ (1.10 g, 5 mmol) in the same solvent (25 cm^3) was added solid $Ag(O_2CMe)$ (1.67 g, 10 mmol) and the AgCl formed after stirring was filtered out to leave solution B. Solution B was added with stirring to A and stirring was continued for 1 d. After 2 d of standing, well formed crystals were observed; this first batch was filtered out {Found: C, 35.2; N, 4.0; H, 5.6. Calc. for $[SnMe_2(H_2O)(PN - 2H)]\cdot 0.5H_2O$: C, 35.0; N, 4.1; H, 5.5%}. M.p. >300 °C. Yield (first batch) 18%. Main metallated signals in the EI mass spectrum: *m*/*z* 299 {$[SnMe_2(PN - 2H - OH)]$, 42.2}, 285 {$[SnMe_2(PN - 2H - CH_2OH)]$, 15.7}, 150 ($[SnMe_2]$, 65.8), 135 ([SnMe], 54.9) and 120 ([Sn], 37.5%). Besides these the spectrum showed signals for pyridoxine and its fragments, and the FAB spectrum signals at 632 ($[\{SnMe_2(PN - 2H)\}_2]$, 2.6) and 317 {$[SnMe_2(PN - H)]$, 4.9%}. Infrared and Raman (in parentheses), cm^{-1}: 1678m, 1640m, 1617w, δ(OH); 1588m (1587w), 1556m (1557w), 1532m, ν(ring); 1025vs (br), ν(CO); 569m (571m), ν_{asym}(Sn–C); 525 (sh) (523vs), ν_{sym}(Sn–C). Λ_M (dmso) 0.3 S cm^2 mol^{-1}.

Crystallography

Crystallography for compounds **1–3** was performed at 293 K with an Enraf-Nonius CAD4 diffractometer and graphite-

Table 1 Molar quantities of NO_3^-, Cl^- and $MeCO_2^-$ present in reactions affording compounds **1**, **2** or **3**, relative to the quantity of $SnMe_2^{2+}$

$[SnMe_2^{2+}]$	[PN]	$[NO_3^-]$	$[Cl^-]$	$[MeCO_2^-]$	Compound prepared
1	2	0	4	0	**2** $[SnMe_2(H_2O)(PN - H)]Cl{\cdot}H_2O$
1	2	1	3	0	**2**
1	2	2	2	0	Random
1	2	3	1	0	**1** $[SnMe_2(PN - H)]NO_3{\cdot}2H_2O$
1	2	4	0	0	**1**
1	2	0	2	2	**2**
1	2	0	3	1	**2**
1	2	2	0	2	**3** $[SnMe_2(H_2O)(PN - 2H)]{\cdot}0.5H_2O$
1	2	3	0	1	**1**

monochromated Mo-Kα radiation (λ = 0.710 73 Å). Unit-cell dimensions were determined by least-squares refinement on diffractometric angles for 25 automatically centred reflections ($11 < \theta < 23$ **1**, $11 < \theta < 23$ **2**, $9 < \theta < 23°$ **3**). Intensities were measured in ω–2θ mode with ω-scan width 0.8 + 0.35 tan θ **1**, **2** or 1.0 + 0.35 tan θ **3**, and were corrected for Lorentz-polarization effects. Absorption corrections[13] were applied at a later stage in the refinement with maximum and minimum factors 1.18 and 0.80 **1**, 1.10 and 0.84 **2** and 1.12 and 0.86 **3**.

The structures were solved by the standard heavy-atom Patterson method followed by normal Fourier-difference techniques. Blocked-matrix least-squares refinement was performed with all non-H atoms anisotropic; hydrogen atoms included in the model, as fixed contributors, were those found in difference syntheses, which were all assigned a common isotropic thermal parameter that refined to $U_{iso} = 0.064(4)$ **1**, 0.071(2) **2** or 0.090(6) Å^2 **3**. The function minimized was $\Sigma w(|F_o| - |F_c|)^2$ with the weighting scheme $w = 1/[\sigma^2(F_o) + 0.0001F_o^2]$ for **1** and **2** and $w = 1/[\sigma^2(F_o) + 0.0003F_o^2]$ for **3**. Final Fourier maps showed no features of chemical significance. The programs used were SHELX 76,[14] ORTEP[15] and SCHAKAL.[16] For non-H atoms scattering factors were taken from Cromer and Mann[17] with corrections for anomalous dispersion from Cromer and Liberman[18] and for H atoms from Stewart *et al.*[19] The crystal data and experimental details are summarized in Table 2.

CCDC reference number 186/678.

Results and Discussion

Synthesis

Crystals of compounds **1–3** for X-ray diffraction studies were synthesized as described in the Experimental section. In addition, they were also synthesized using other quantities of $AgNO_3$ and/or $Ag(O_2CMe)$ in solutions A and B so as to procure other relative amounts of NO_3^-, Cl^- and $MeCO_2^-$ in the reaction mixture (Table 1); the products of these reactions were characterized by chemical analysis and IR and ^{1}H NMR spectrometry. In each case, after the first batch of solid was separated from the mother-liquor, further concentration led to the formation of impure solids which, especially in the case of **3**, contained crystallized protonated pyridoxine. When the mole ratio of X^- (Cl^-, NO_3^-) to $MeCO_2^-$ was 1:3 or 0:4 the first-batch solids were white and have not yet been identified. The following features of Table 1 deserve comment.

(*i*) To promote deprotonation of PN it was used in excess (in the presence of NO_3^- or Cl^- ions the excess of PN will have captured the protons released from the PN molecules acting as ligands). The $MeCO_2^-$ anion was used as an additional proton capturer.

(*ii*) The solid isolated from asymmetric NO_3^-/Cl^- systems contained the major anion of the solution; when the $NO_3^-:Cl^-$ mole ratio was 2:2 the solid isolated contained random amounts of Cl^- and NO_3^-.

(*iii*) The Cl^-–$MeCO_2^-$ and NO_3^-–$MeCO_2^-$ systems afforded solids with pyridoxine in the same monodeprotonated state when the $X^-:MeCO_2^-$ mole ratio (X = Cl, NO_3) was 3:1. However, equimolar (2:2) X^-–$MeCO_2^-$ systems afforded solids in which the ligand was monodeprotonated for X = Cl but dideprotonated for $X = NO_3$. Although it cannot be ruled out that the two media differed as regards the concentrations of $[SnMe_2(PN - H)]^+$ and $[SnMe_2(PN - 2H)]$, it seems likely that the formation of different solids will have been due to their different solubilities in the two media.

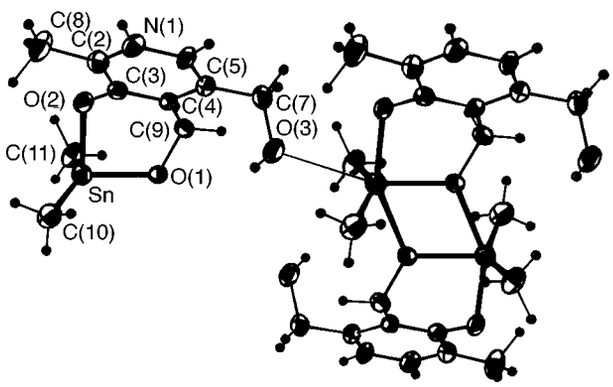

Fig. 1 Crystal structure of $[SnMe_2(PN - H)]NO_3{\cdot}2H_2O$ **1**, showing the numbering scheme (NO_3^- and H_2O have been excluded). Displacement ellipsoids are drawn at the 50% probability level

Structure of $[SnMe_2(PN - H)]NO_3{\cdot}2H_2O$ 1

Fig. 1 shows the structure of compound **1** and the atom-numbering scheme. Selected bond distances and angles are listed in Table 3. Besides the NO_3^- ions and H_2O molecules, the crystal consists of dimeric $[Sn_2Me_4(PN - H)_2]$ units in which the two pyridoxinato anions are both zwitterions (**Ib** in Scheme 1) with deprotonated 4-CH_2OH groups, and both bridge between the Sn atoms. In each dimeric unit each tin atom co-ordinates to the two methyl C atoms, the O(2) of a deprotonated phenolic hydroxyl group, the O(1) of a deprotonated 4-CH_2OH group and the similarly deprotonated O(1^i) of the other pyridoxinato anion. Thus both O(1) and O(1^i) bridge between the two tin atoms to form an Sn_2O_2 ring. This ring is planar, and the distances and angles in it differ little from those found in Sn_2O_2 rings in which deprotonated alcoholic O atoms bridge between $SnCl_2^{2+}$ ions[20,21] or hydroxyl O atoms bridge between two dimethyltin(IV) units.[22,23] The Sn_2O_2 plane makes a dihedral angle of 141° with that of the N(1) to C(6) ring, which is totally planar ($X^2 = 0$). The non-H atoms immediately adjoining the pyridoxine ring [O(2), C(7), C(8) and C(9)] lie practically in the plane of the ring itself, and O(2), which is the farthest from this plane (0.05 Å), is also only 0.054 Å from the Sn_2O_2 plane.

The distorted octahedral co-ordination polyhedron of each tin atom is completed by an O(3) atom belonging to a neighbouring dimer, which results in the formation of $Sn_2O_4C_8$ rings that link the dimers in a polymeric chain along the *b* axis (Fig. 2). The Sn_2O_2 rings in this chain are not coplanar but stepped, the distance between successive Sn_2O_2 planes being 1.711 Å. The Sn–O(3) bond length [2.802(3) Å] is longer than in other

Table 2 Crystal data, data collection and structure refinement parameters

	1 $[SnMe_2(PN - H)]NO_3 \cdot 2H_2O$	**2** $[SnMe_2(H_2O)(PN - H)]Cl \cdot H_2O$	**3** $[SnMe_2(H_2O)(PN - 2H)] \cdot 0.5H_2O$
Formula	$C_{10}H_{20}N_2O_8Sn$	$C_{10}H_{20}ClNO_5Sn$	$C_{10}H_{15}NO_3Sn \cdot 1.5H_2O$
M	414.97	388.42	342.95
Crystal system	Triclinic	Monoclinic	Monoclinic
Space group	$P\bar{1}$ (no. 2)	$P2_1/a$	$P2_1/c$
a/Å	7.1266(8)	11.056(1)	9.168(1)
b/Å	8.1056(8)	11.396(1)	7.498(1)
c/Å	14.523(4)	12.323(2)	19.637(3)
α/°	73.76(2)	—	—
β/°	80.29(2)	110.40(1)	101.39(1)
γ/°	82.58(1)	—	—
U/Å^3	795.3(2)	1455.8(6)	1323.2(6)
Z	2	4	4
D_c/g cm^{-3}	1.73	1.77	1.72
F(000)	416	776	684
μ/mm^{-1}	16.46	19.56	19.40
Reflections measured	2898	2857	2311
Unique reflections, R	2772, 0.033	2733, 0.014	2172, 0.021
Reflections observed [$I > 3\sigma(I)$]	2725	2409	1984
$R = \Sigma(\|F_o\| - \|F_c\|)/\Sigma\|F_o\|$	0.036	0.023	0.032
$R' = [\Sigma w(\|F_o\| - \|F_c\|)^2/\Sigma w\|F_o\|^2]^{\frac{1}{2}}$	0.038	0.025	0.036

Table 3 Bond distances (Å) and angles (°) in $[SnMe_2(PN - H)]NO_3 \cdot 2H_2O$ **1** with estimated standard deviations (e.s.d.s) in parentheses

(*a*) Tin environment[a]

Sn–O(1)	2.063(3)	Sn–C(11)	2.100(5)
Sn–O(2)	2.104(3)	Sn–O(1^{i})	2.291(3)
Sn–C(10)	2.104(5)	Sn–O(3^{ii})	2.802(3)
O(1)–Sn–O(2)	84.1(1)	O(2)–Sn–O(1^{i})	153.2(1)
O(1)–Sn–C(10)	106.1(2)	C(10)–Sn–C(11)	143.8(2)
O(1)–Sn–C(11)	106.4(2)	C(10–Sn–O(3^{ii})	78.5(2)
O(1)–Sn–O(3^{ii})	160.6(1)	C(10)–Sn–O(1^{i})	87.9(2)
O(1)–Sn–O(1^{i})	69.1(1)	C(11)–Sn–O(3^{ii})	76.0(2)
O(2)–Sn–C(10)	98.6(2)	C(11)–Sn–O(1^{i})	89.4(2)
O(2)–Sn–C(11)	100.0(2)	O(3^{ii})–Sn–O(1^{i})	130.3(1)
O(2)–Sn–O(3^{ii})	76.5(1)		

(*b*) Pyridoxine ligand

O(1)–C(9)	1.419(6)	O(2)–C(3)	1.338(5)
O(3)–C(7)	1.400(6)	N(1)–C(2)	1.335(6)
N(1)–C(6)	1.348(6)	C(2)–C(3)	1.398(6)
C(2)–C(8)	1.489(7)	C(3)–C(4)	1.388(6)
C(4)–C(5)	1.410(6)	C(4)–C(9)	1.498(6)
C(5)–C(6)	1.382(6)	C(5)–C(7)	1.509(7)
C(2)–N(1)–C(6)	123.6(4)	C(3)–C(4)–C(9)	118.0(4)
N(1)–C(2)–C(3)	118.2(4)	C(5)–C(4)–C(9)	122.4(4)
N(1)–C(2)–C(8)	118.4(4)	C(4)–C(5)–C(6)	117.9(4)
C(3)–C(2)–C(8)	123.4(4)	C(4)–C(5)–C(7)	123.7(4)
O(2)–C(3)–C(2)	118.6(4)	C(6)–C(5)–C(7)	118.4(4)
O(2)–C(3)–C(4)	121.1(4)	N(1)–C(6)–C(5)	120.4(4)
C(2)–C(3)–C(4)	120.2(4)	O(1)–C(9)–C(4)	110.4(4)
C(3)–C(4)–C(5)	119.6(4)	O(3)–C(7)–C(5)	112.3(4)

(*c*) Nitrate ion

N(2)–O(4)	1.231(6)	O(4)–N(2)–O(5)	120.4(5)
N(2)–O(6)	1.236(6)	O(4)–N(2)–O(6)	119.4(4)
N(2)–O(5)	1.246(6)	O(5)–N(2)–O(6)	120.2(5)

(*d*) Hydrogen bonds[b]

O(3)···O(w1^{i})	2.671(6)	O(3)–H(O3)–O(w1^{i})	176.2(3)
H(O3)–O(w1^{i})	1.631(6)		
N(1)···O(4^{ii})	2.768(7)	N(1)–H(N1)–O(4^{ii})	174.2(3)
H(N1)–O(4^{ii})	1.838(7)		
O(6)···O(w2^{iii})	2.841(8)	O(w2^{iii})–H(Ow2^{iii})–O(6)	166.6(4)
O(6)–H(Ow2^{iii})	2.045(8)		
O(w1)···O(w2^{iv})	2.793(8)	O(w1)–H(Ow1)–O(w2^{iv})	163.8(4)
H(Ow1)–O(w2^{iv})	1.861(8)		

[a] Symmetry operations: i $1 - x, -y, -z$; ii $x, 1 + y, z$. [b] Symmetry operations: i $1 - x, -1 - y, -z$; ii $1 - x, -y, -1 - z$; iii $1 - x, -y, -z$; iv $1 + x, y, z$.

alcohol complexes of tin[24] and much longer than Sn–O(1), which is the normal length for a covalent bond (the sum of the covalent radii of Sn and O is 2.13 Å[25]), but Sn–O(3) is shorter than the sum of the van der Waals radii (3.70 Å[25]) and is in the range that has confidently been reported to indicate Sn–O bonding.[26]

The main geometric features of $(PN - H)^-$ in compound **1** (Table 3), particularly the C(9)–O(1) and C(3)–O(2) bond lengths [1.419(6) and 1.338(5) Å respectively], agree well with those in other complexes[9b] in which, as in **1**, it chelates *via* its deprotonated phenolic hydroxyl and 4-CH_2OH groups. Comparison with free PN[27] shows that deprotonation of the phenolic hydroxyl group has a negligible effect on the C(2)–C(3)–C(4) angle [120.2(4)° in **1** as against 120.3(3)° in pyridoxine] but shortens C(3)–O(2) from 1.374(4) to 1.338(5) Å. The C(9)–O(1) distance is practically unmodified [1.419(6) *vs.* 1.391(5) Å in PN] but the C(2)–N(1)–C(6) angle is widened from 119.3(3) to 123.6(4)°, a value close to the 124.7(2)° found in PN·HCl,[28] in which, as in **1**, the N atom is protonated. The geometry of the C(5)–CH_2OH fragment is similar to that observed in structures in which other metals co-ordinate to monodeprotonated pyridoxine *via* O(1) and O(2), leaving C(5)–CH_2OH to take part in hydrogen bonds.[9b]

Hydrogen bonds shown by their structural parameters to be moderately strong (Table 3) are formed between O(3) and a water molecule, and between the N(1)–H group and a nitrate group oxygen [O(4)]. There are also weaker hydrogen bonds between another nitrate oxygen [O(6)] and a water molecule, and between two water molecules. All these bonds (some of which are represented in Fig. 3) help stabilize the packing in the crystal.

Structure of $[SnMe_2(H_2O)(PN - H)]Cl \cdot H_2O$ 2

Fig. 4 shows the atomic arrangement of compound **2** and its numbering scheme. Selected bond distances and angles are listed in Table 4. The crystal consists of centrosymmetric $[Sn_2Me_4(PN - H)_2(H_2O)_2]$ dimers, chloride ions and H_2O molecules. Within each dimer, the Sn(PN − H) co-ordination scheme is identical to that found in **1**, and the two compounds show no marked differences as regards interatomic distances and angles in the ligand. The Sn_2O_2 ring is slightly more asymmetric in **1** than in **2**, and the Sn–O(2) bond slightly longer in **2** than in **1**.

In compound **2** the co-ordination polyhedron of the tin atom is completed within the dimeric unit by a water molecule, which thus prevents the polymerization found in **1**. Although the

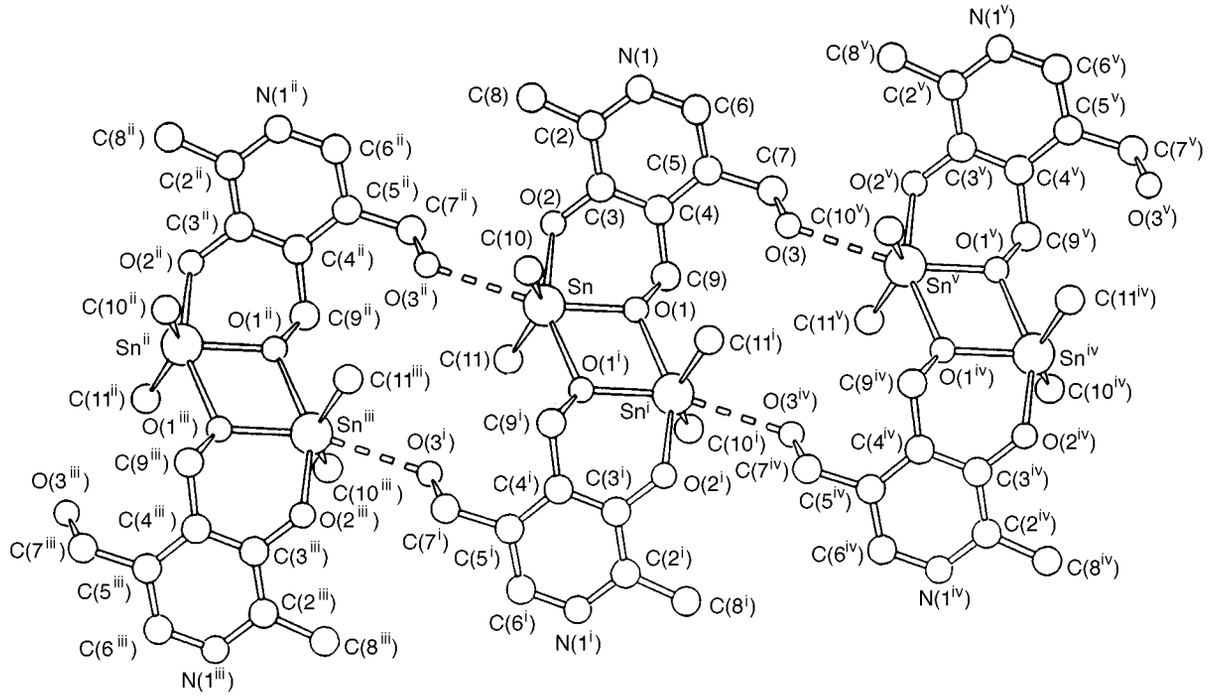

Fig. 2 Polymeric structure of compound **1** (NO_3^- and H_2O have been excluded)

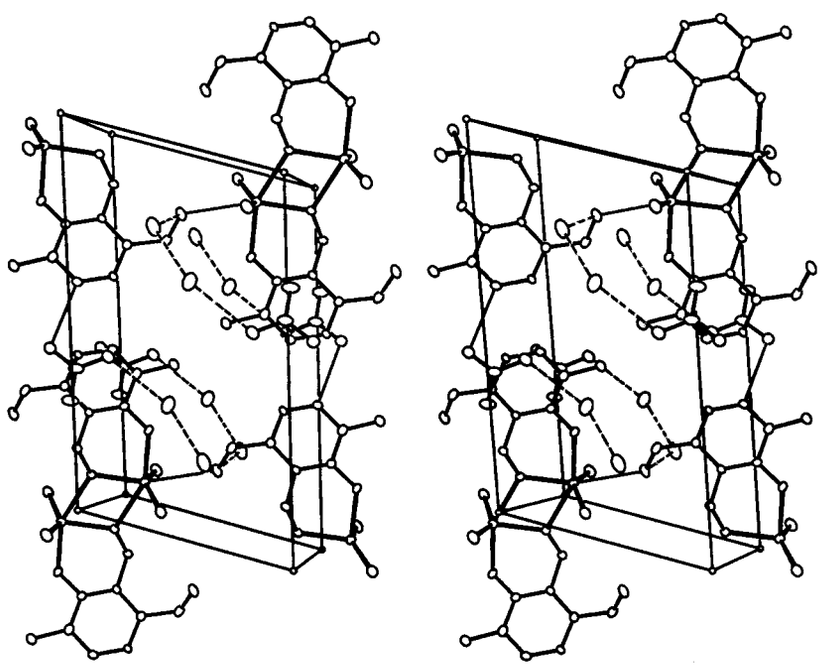

Fig. 3 Packing arrangement in crystalline compound **1**, showing the hydrogen bonds

polyhedron is a distorted octahedron in both **1** and **2**, the two compounds have different bond lengths and angles around the tin atom. The Sn–C bond lengths are similar, but the Sn–O distances differ [in particular, the Sn–O(w2) distance of 2.466(3) Å in **2** is much shorter than the Sn–O(3^{ii}) distance of 2.802(3) Å in **1**]. As in **1**, angular distortion in the equatorial SnO_4 plane mainly affects the oxygen that does not belong to a PN − H ligand in the same dimer as Sn, O(w2) in this case; the difference between the distortions in **1** and **2** may probably be attributed to the formation of a polymeric arrangement in **1**. The C–Sn–C angle is slightly wider in **2** than in **1**, probably because the Sn–O(w2) distance in **2** is much shorter than the Sn–O(3^{ii}) distance in **1**.

The co-ordinated water molecule interacts with the unco-ordinated water molecule through a hydrogen bond stronger than any of those present in compound **1** (*cf.* Tables 3 and 4). A slightly weaker intermolecular hydrogen bond involves the phenolic O and the unco-ordinated water molecule. These bonds and the packing arrangement in the crystal are shown in Fig. 5. The co-ordinated and unco-ordinated water molecules are also both involved in hydrogen bonds with the chloride ion.

Structure of $[SnMe_2(H_2O)(PN - 2H)]\cdot 0.5H_2O$ 3

The structure and atom numbering scheme of compound **3** are shown in Fig. 6, and selected bond lengths and angles are listed in Table 5. The crystal is formed of dimeric $[Sn_2Me_4(PN - 2H)_2(H_2O)_2]$ units together with water of crystallization $[O(w2)H_2]$ that exhibits 'ordered disorder', the occupation

Table 4 Bond distances (Å) and angles (°) in $[SnMe_2(H_2O)(PN - H)]Cl\cdot H_2O$ **2**, with e.s.d.s in parentheses

(*a*) Tin environment[a]

Sn–O(1)	2.116(2)	Sn–C(10)	2.109(4)
Sn–O(1^i)	2.203(2)	Sn–C(11)	2.093(4)
Sn–O(2)	2.179(2)	Sn–O(w2)	2.466(3)
O(1)–Sn–O(2)	83.30(8)	O(2)–Sn–O(1^i)	154.71(8)
O(1)–Sn–C(10)	96.9(1)	C(10)–Sn–C(11)	159.9(1)
O(1)–Sn–C(11)	103.2(11)	C(10)–Sn–O(w2)	81.6(1)
O(1)–Sn–O(w2)	162.09(9)	C(10)–Sn–O(1^i)	95.2(1)
O(1)–Sn–O(1^i)	72.02(8)	C(11)–Sn–O(w2)	79.7(1)
O(2)–Sn–C(10)	93.2(1)	C(11)–Sn–O(1^i)	92.2(1)
O(2)–Sn–C(11)	88.0(1)	O(w2)–Sn–O(1^i)	90.28(8)
O(2)–Sn–O(w2)	114.57(9)		

(*b*) Pyridoxine ligand

O(1)–C(9)	1.431(4)	C(2)–C(8)	1.488(5)
O(2)–C(3)	1.323(4)	C(3)–C(4)	1.409(4)
O(3)–C(7)	1.413(4)	C(4)–C(5)	1.400(4)
N–C(2)	1.351(4)	C(4)–C(9)	1.514(4)
N–C(6)	1.343(4)	C(5)–C(6)	1.379(4)
C(2)–C(3)	1.396(4)	C(5)–C(7)	1.514(5)
C(2)–N–C(6)	124.1(3)	C(3)–C(4)–C(9)	117.4(3)
N–C(2)–C(3)	118.1(3)	C(5)–C(4)–C(9)	122.4(3)
N–C(2)–C(8)	118.6(3)	C(4)–C(5)–C(6)	118.4(3)
C(3)–C(2)–C(8)	123.3(3)	C(4)–C(5)–C(7)	121.7(3)
O(2)–C(3)–C(2)	119.0(3)	C(6)–C(5)–C(7)	119.9(3)
O(2)–C(3)–C(4)	121.7(3)	N–C(6)–C(5)	120.1(3)
C(2)–C(3)–C(4)	119.2(3)	O(3)–C(7)–C(5)	114.1(3)
C(3)–C(4)–C(5)	120.1(3)	O(1)–C(9)–C(4)	111.3(3)

(*c*) Hydrogen bonds[b]

O(w1)···O(w2)	2.666(4)	O(w1)–H(w2)–O(w2)	165.8(2)
O(w1)–H(w2)	1.705(3)		
Intermolecular			
O(2)···O(w1^i)	2.907(4)	O(w1^i)–H(w1^i)–O(2)	163.9(2)
O(2)–H(w1^i)	1.958(2)		
Interactions around the Cl ion			
Cl···O(w1)	3.247(4)	Cl···O(w2)	3.167(3)
Cl···H′(w1)	2.4773(9)	Cl···H′(w2)	2.2449(9)
O(w1)–H′(w1)–Cl	150.1(2)	O(w2)–H′(w2)–Cl	172.4(2)

[a] Symmetry operation: i $-x$, $1 - y$, $-z$. [b] Symmetry operation: i $\frac{1}{2} - x$, $y - \frac{1}{2}$, $-z$.

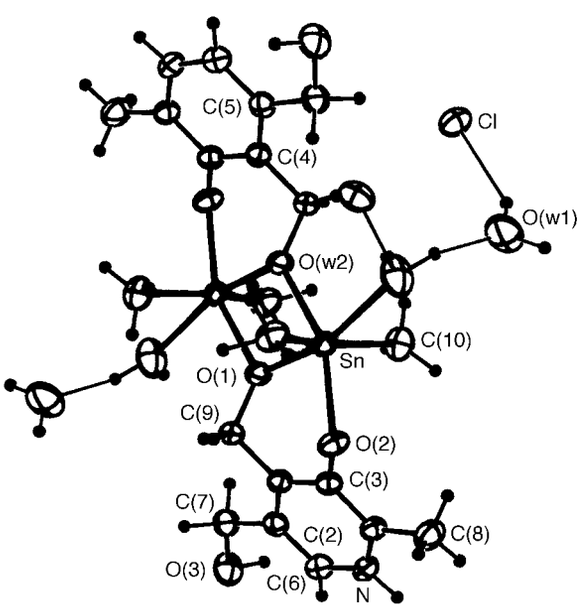

Fig. 4 Crystal structure of $[SnMe_2(H_2O)(PN - H)]Cl\cdot H_2O$ **2**, showing the numbering scheme. Displacement ellipsoids are drawn at the 50% probability level

Table 5 Bond distances (Å) and angles (°) in $[SnMe_2(H_2O)(PN - 2H)]\cdot 0.5H_2O$ **3**, with e.s.d.s in parentheses

(*a*) Tin environment[a]

Sn–O(1)	2.046(4)	Sn–C(11)	2.105(6)
Sn–O(2)	2.087(3)	Sn–O(1^i)	2.268(3)
Sn–C(10)	2.088(6)	Sn–O(w1)	2.963(5)
O(1)–Sn–O(2)	85.6(1)	O(2)–Sn–O(1^i)	154.7(1)
O(1)–Sn–C(10)	108.9(2)	C(10–Sn–C(11)	142.2(2)
O(1)–Sn–C(11)	106.0(2)	C(10)–Sn–O(w1)	74.3(2)
O(1)–Sn–O(w1)	164.0(1)	C(10)–Sn–O(1^i)	88.6(2)
O(1)–Sn–O(1^i)	69.2(1)	C(11)–Sn–O(w1)	76.0(2)
O(2)–Sn–C(10)	96.9(2)	C(11)–Sn–O(1^i)	90.6(2)
O(2)–Sn–C(11)	99.7(2)	O(w1)–Sn–O(1^i)	126.7(1)
O(2)–Sn–O(w1)	78.4(1)		

(*b*) Pyridoxine ligand

O(1)–C(9)	1.428(6)	C(2)–C(8)	1.513(8)
O(2)–C(3)	1.333(6)	C(3)–C(4)	1.397(7)
O(3)–C(7)	1.417(6)	C(4)–C(5)	1.387(7)
N–C(2)	1.314(7)	C(4)–C(9)	1.508(7)
N–C(6)	1.338(7)	C(5)–C(6)	1.376(7)
C(2)–C(3)	1.400(7)	C(5)–C(7)	1.518(7)
C(2)–N–C(6)	119.0(5)	C(3)–C(4)–C(9)	117.6(4)
N–C(2)–C(3)	122.0(5)	C(5)–C(4)–C(9)	123.9(4)
N–C(2)–C(8)	118.2(5)	C(4)–C(5)–C(6)	118.3(5)
C(3)–C(2)–C(8)	119.8(5)	C(4)–C(5)–C(7)	122.5(4)
O(2)–C(3)–C(2)	120.1(4)	C(6)–C(5)–C(7)	119.2(5)
O(2)–C(3)–C(4)	121.0(4)	N–C(6)–C(5)	123.4(5)
C(2)–C(3)–C(4)	118.8(4)	O(3)–C(7)–C(5)	113.6(4)
C(3)–C(4)–C(5)	118.5(4)	O(1)–C(9)–C(4)	110.6(4)

(*c*) Hydrogen bonds[b]

(*i*) Intramolecular

O(2)···O(w2)	2.891(9)	O(w1)–H(Ow1)	1.028(4)
O(w1)···O(w2)	2.759(9)	O(w2)–H(Ow1)	1.811(9)
O(w1)–H(Ow1)–O(w2)	151.7(4)		

(*ii*) Intermolecular

O(w1)···O(w2^i)	2.76(1)	O(w2^i)···H(Ow1)	1.878(9)
O(w2)···O(w2^i)	1.44(1)		
O(w1)–H(Ow1)–O(w2^i)	141.4(3)		
O(3)···N^{ii}	2.710(6)	O(3)···H(O3)	0.903(4)
N^{ii}···H(O3)	1.832(5)		
O(3)–H(O3)–N^{ii}	163.6(3)		

[a] Symmetry operation: i $1 - x$, $-y$, $1 - z$. [b] Symmetry operations: i $1 - x$, $1 - y$, $1 - z$; ii $1 - x$, $y - \frac{1}{2}$, $\frac{3}{2} - z$.

number of the oxygen atom being $\frac{1}{2}$. In Fig. 6, the two possible positions of O(w2) are shown together with the corresponding intramolecular hydrogen bonds.

In the dimer unit each tin atom is co-ordinated octahedrally as in compounds **1** and **2**. The geometrical parameters of the dimer unit are similar to those of **1**; in fact, if the tin methyl groups are excluded, application of the Kabsch method[29] to the dimer units of **1** and **3** shows a root-mean-square deviation between homologous atoms of only 0.07 Å. The Sn–O(w1) distance is longer in **3** than in **2** (probably because of the greater negative charge of the pyridoxinate ligand) but is nevertheless within the reported range for Sn–O bonding.[26]

The main structural differences between the PN − 2H ligand in compound **3** and the PN − H ligand of **1** and **2** lie in the vicinity of the deprotonation site, N. Deprotonation of PN − H to PN − 2H slightly shortens the N–C(2) and N–C(6) bond lengths, narrows the angle C(2)–N–C(6) by about 5°, and slightly widens N–C(2)–C(3) and N–C(6)–C(5), just as deprotonation of PN·HCl to PN does.[27,28]

The hydrogen-bond pattern in compound **3** is slightly more

Table 6 Solid-state ^{13}C NMR spectral data (δ)

Compound	C(3)	C(2)	C(6)	C(4)	C(5)	C(7)	C(9)	C(8)	Sn–CH_3
PN	151.4	145.4	134.5	132.5	128.5	59.9	59.9	17.4	
PN·HCl	153.4	141.9	125.1	141.9	136.4	62.6	59.6	16.7	
$[SnMe_2(PN - H)]NO_3·2H_2O$	158.6	146.4	130.4	146.4	133.9	59.6	59.6	14.8	7.9
									6.2
$[SnMe_2(H_2O)(PN - H)]Cl·H_2O$	159.6	145.0	121.4	142.3	138.0	59.3	59.3	13.7	12.1
									9.9
$[SnMe_2(H_2O)(PN - 2H)]·0.5H_2O$*	158.7	151.3	130.4	146.3	137.7	59.9	58.2	17.4	7.8
	157.3	150.0	128.2	145.2	136.8			14.8	6.2
	156.6				135.2			13.2	5.7
					134.4				4.8
					133.1				
					132.2				

* Data obtained at 12 kHz using a Bruker DSX 500 spectrometer with a high-speed rotor.

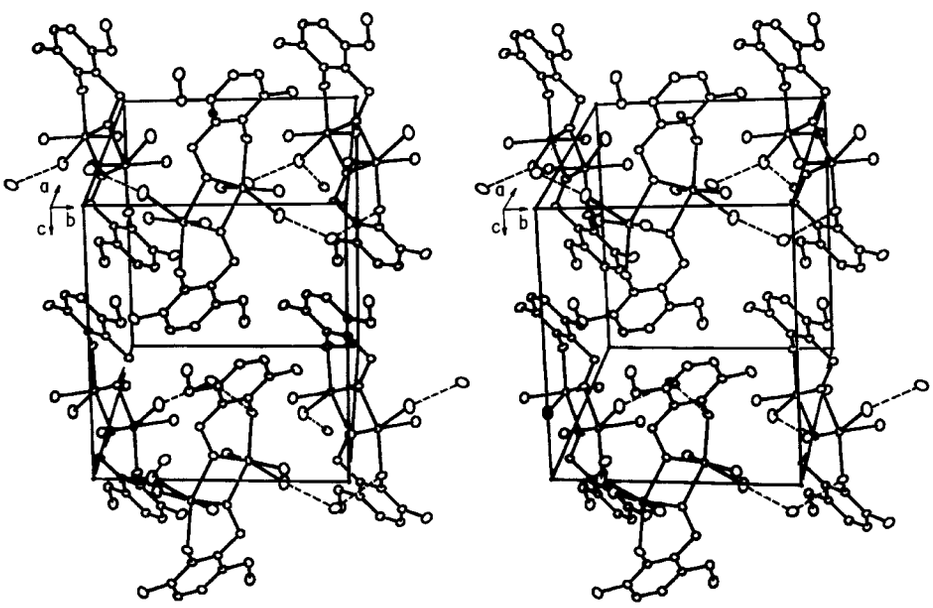

Fig. 5 Packing arrangement in crystalline compound **2**, showing the hydrogen bonds

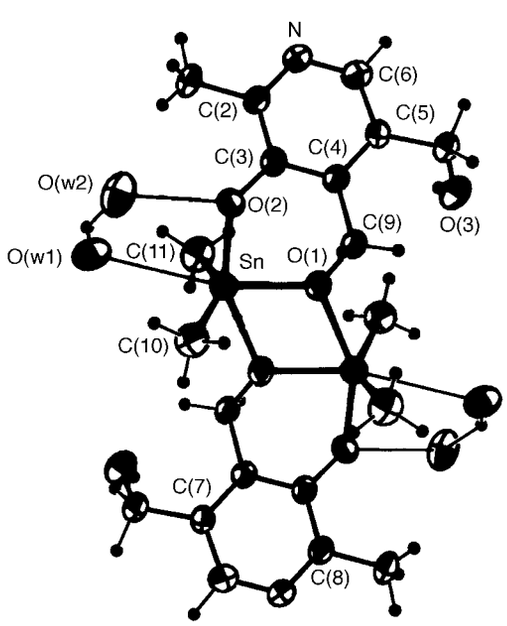

Fig. 6 Crystal structure of $[SnMe_2(H_2O)(PN - 2H)]·0.5H_2O$ **3**, showing the numbering scheme. Displacement ellipsoids are drawn at the 50% probability level

complex than in **1** and **2**. The O(2)···O(w) and O(w)···O(w) hydrogen bonds are present as before, but there is also a moderately strong hydrogen bond between the 5-CH_2OH group and the N atom of a neighbouring molecule (Table 5). Fig. 7 shows the packing in the crystal.

Vibrational spectra

Besides the bands indicated in the Experimental section, the IR spectra of all these compounds exhibit two sets of medium-strong bands located near 3300 and 2800 cm^{-1} {one at 3496, 3424, 3367 and 3327 and the other at 2897, 2864 and 2811 cm^{-1} in the case of $[SnMe_2(H_2O)(PN - H)]Cl·H_2O$}. These bands are jointly attributed to ν(OH) of the 5-CH_2OH group, ν(OH) of co-ordinated or lattice water, and ν(N–H) of the NH group when this is present; individual assignment was prevented by the slight shifts caused by the involvement of the corresponding groups in hydrogen bonds and/or co-ordination. The range 1650–1450 cm^{-1} shows the pyridine ring bands and, as previously reported,[30] in the spectra of the N-protonated compounds this region also shows a strong band at about 1530 cm^{-1} [probably contributed to by ν(C–O) of the co-ordinated ≥C–O^- group] and two weak Raman bands near 1600 cm^{-1}. In the spectra of **3** these two bands do not appear and the 1530 cm^{-1} band is less intense.

A strong band close to 1020 cm^{-1} in the spectrum of compound **3** and close to 1000 cm^{-1} in the N-protonated complexes has been attributed[31] to ν(C–O) of the 5-CH_2OH group. These bands are close to the positions of this ν(C–O) vibration for PN (1023s, IR) and PN·HCl (1019s, IR), the biggest shift being shown by $[SnMe_2(PN - H)]NO_3·2H_2O$; although this shift may be due to the co-ordination of the 5-CH_2OH oxygen to tin, this

Table 7 Proton and ^{13}C NMR data in dmso solution[a]

Compound	δ H(6)	H(O3)	H(9)	H(7)	H(8)	Sn–CH_3	$^2J(^1H–^{119}Sn)$/Hz	θ(C–Sn–C)/° NMR[b]	X-Ray data
PN	8.17 (s, 1)[c]	5.21 (s, br)	4.76 (s, 2)	4.50 (s, 2)	2.34 (s, 3)				
PN·HCl	8.11 (s, 1)	5.64 (s, br)	4.77 (s, 2)	4.70 (s, 2)	2.59 (s, 3)				
$[SnMe_2(PN - H)]NO_3·2H_2O$	7.83 (s, 1)	5.50 (s, br)	4.83 (s, 2)	4.56 (s, 2)	2.40 (s, 3)	0.63	90.4	144.8	143.8
$[SnMe_2(H_2O)(PN - H)]Cl·H_2O$	7.76 (s, 1)	5.14 (s, br)	4.75 (s, 2)	4.49 (s, 2)	2.33 (s, 3)	0.76	98.1	158.8	159.9
$[SnMe_2(H_2O)(PN - 2H)]·0.5H_2O$	7.73 (s, 1)	5.25 (s, br)	4.83 (s, 2)	4.49 (s, 2)	2.34 (s, 3)	0.58	86.3	139.4	142.2
	C(3)	C(2)	C(6)	C(4)	C(5)	C(7)	C(9)	C(8)	Sn–CH_3
PN	149.9	146.1	138.9	133.3	131.5	59.0	56.8	19.3	
PN·HCl	151.8	140.8	128.6	141.3	138.8	57.6	55.4	14.6	
$[SnMe_2(PN - H)]NO_3·2H_2O$	158.8 (br)	143.3	126.0 (br)	143.3 (br)	136.1	58.2	57.9	14.9	7.6 (br)

[a] s = Singlet, br = broad. [b] $\theta = 0.016|^2J|^2 - 1.32|^2J| + 133.4$. [c] Relative numbers of protons calculated by integration in parentheses.

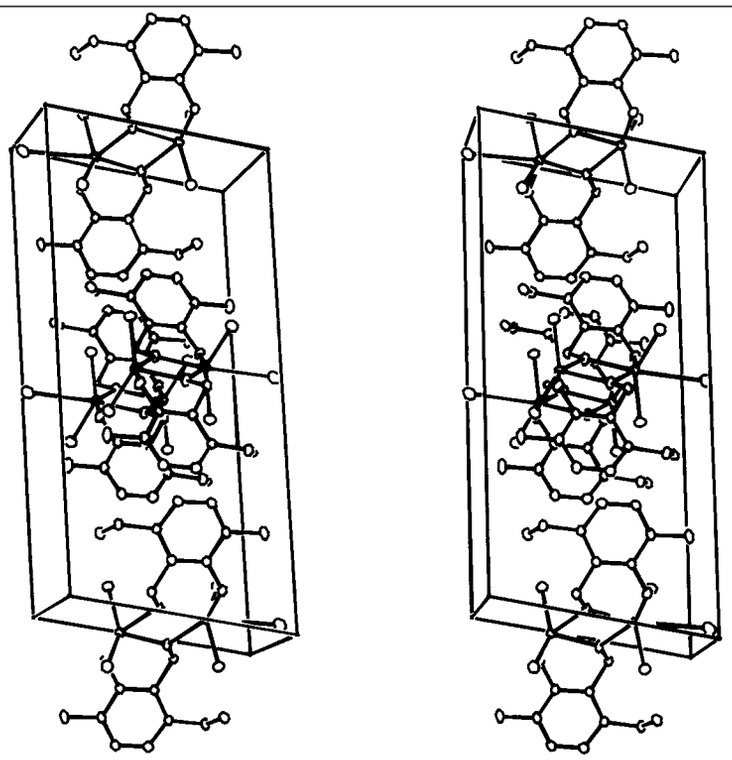

Fig. 7 Packing arrangement in crystalline compound **3**

is still an open question in view of the weakness of the Sn–O interaction, the differences between **1** and free PN as regards hydrogen bonding, and previous data.[32] Several medium bands at slightly higher and lower wavenumbers in the spectra of all three compounds may be due to ν(C–O) of the co-ordinated 4-CH_2O^- group, but the presence of pyridine bands in this region prevents definite assignment.

The non-linearity of the C–Sn–C fragment (confirmed by X-ray diffraction) is shown by the presence of ν_{asym}(Sn–C) and ν_{sym}(Sn–C) in the IR and Raman spectra of all three compounds.

NMR spectra

***(a)* Solid state.** The solid-state ^{13}C cross polarization magic angle spinning (CP MAS) NMR data of PN, PN·HCl and the complexes are given in Table 6. Most of the carbons generate separate signals, which were assigned on the basis of previously published[11] data and the results obtained in dmso solution (see below). The protonation of PN strongly deshields C(4) and C(5), strongly shields C(6), and only slightly affects the remaining C atoms. In the complexes the co-ordination through O(1) and O(2) observed in the X-ray study deshields C(3) and C(4) with respect to the PN ligand regardless of its protonation status. The presence in compound **1**, but not **2**, of a weak intermolecular interaction between O(3) and the tin atom, which was detected in the X-ray study, may explain the difference between the behaviours of C(5) in these two compounds; note, however, that the C(7) signal seems to be insensitive to the presence of the O(3)···Sn interaction.

The signals at high field are assigned to the methyl groups of the organometallic moiety. The presence, in the spectra of compounds **1** and **2**, of two peaks for the tin methyl groups shows the two groups to be magnetically different in these compounds. The difference between **1** and **2** as regards the chemical shifts of these signals may be related to the fact that although both complexes have the same arrangement around the metallic atom, the natures of the oxygen atoms co-ordinating to the tin atom are different. The spectrum of **3**, which was obtained at high speed and 500 MHz, not only shows the inequivalence of the tin methyls but also distinguishes other carbon atoms. In particular, the broad signal that for PN·HCl and **1** represents both C(2) and C(4), now splits in two, showing C(2) to be the more deshielded (possibly because the ligand in **3** is dideprotonated).

***(b)* Solution.** Table 7 lists ^1H and ^{13}C NMR data for PN, PN·HCl and the complexes in $(CD_3)_2SO$. The signals of PN have been assigned on the basis of previously published

Table 8 Proton and ^{13}C NMR data in D_2O solution[a]

Compound	δ H(6)	H(9)	H(7)	H(8)	Sn–CH_3	^2J(H–Sn)/Hz
PN	7.55 (s, 1)	4.75 (s, 2)	4.64 (s, 2)	2.36 (s, 3)		
PN·HCl	8.18 (s, 1)	5.02 (s, 2)	4.82 (s, 2)	2.66 (s, 3)		
$[SnMe_2(PN - H)]NO_3 \cdot 2H_2O$	7.96 (s, 1)	4.97 (s, 2)	4.82 (s, 2)	2.59 (s, 3)	0.84 (s, 6)	86.6
$[SnMe_2(H_2O)(PN - H)]Cl \cdot H_2O$	7.97 (s, 1)	4.99 (s, 2)	4.81 (s, 2)	2.59 (s, 3)	0.85 (s, 6)	87.3 85.4
$[SnMe_2(H_2O)(PN - 2H)] \cdot 0.5H_2O$	8.01 (s, 1)	5.03 (s, 2)	4.87 (s, 2)[b]	2.65 (s, 3)	0.91 (s, 6)	87.9 84.3

	δ C(3)	C(2)	C(6)	C(4)	C(5)	C(7)	C(9)	C(8)	Sn–CH_3
PN	159.8	144.4	126.0	138.3	135.5	59.0	56.3	15.9	
PN·HCl	154.0	144.0	131.3	142.0	138.1	59.5	58.5	15.7	
$[SnMe_2(PN - H)]NO_3 \cdot 2H_2O$	158.0	144.5	127.4	144.5	135.3	58.6	58.0	14.6	4.3
$[SnMe_2(H_2O)(PN - H)]Cl \cdot H_2O$	157.9	144.6	127.6	144.6	135.3	58.6	58.1	14.6	4.6
$[SnMe_2(H_2O)(PN - 2H)] \cdot 0.5H_2O$	158.2	144.5	127.4	144.5	135.5	58.7	57.9	14.8	4.1

[a] s = Singlet; relative numbers of protons calculated by integration in parentheses. [b] Overlapping the HDO signal.

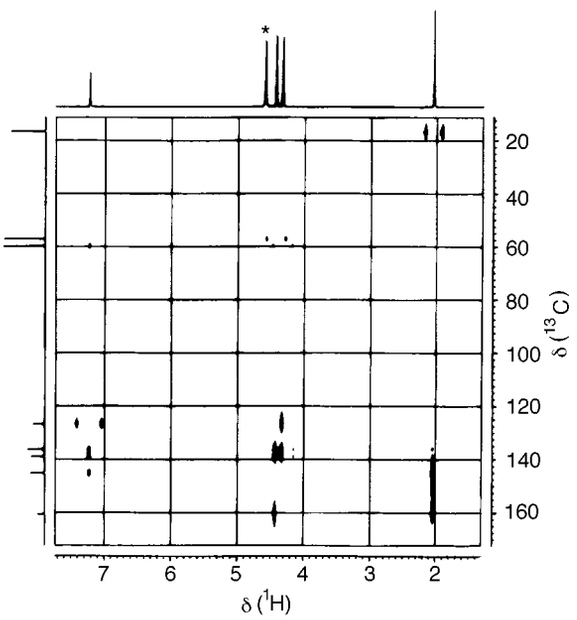

Fig. 8 Two-dimensional $^1H-^{13}C$ HMBC spectrum of PN in D_2O solution, recorded at 500.13 MHz. The asterisk indicates the solvent peak

data;[12b,c] in the absence of sufficient published data about the spectra of PN·HCl in this solvent, we carried out $^1H-^{13}C$ HMBC and HMQC experiments, as previously for PN.[12b,c] Protonation of PN causes slight shielding of H(6) and deshielding of all other protons, while C(3), C(4) and C(5) are deshielded and the other C atoms are shielded [in particular, the C(6) signal moves to higher field than the C(4) and C(5) signals]. The ring signals are close to their positions in the solid-state NMR spectra; however, for PN·HCl the signals of the exocyclic carbons C(7) and C(9) undergo shifts of about 5 ppm which may be related to packing effects in the solid.

Complexation shielded H(6), H(O3), H(7) and H(8) and deshielded H(9), as found previously.[12b,c] This behaviour suggests that, to an appreciable extent, co-ordination through O(1) and O(2) remains in solution. This is confirmed by the good agreement between the values of the C–Sn–C angle observed in the X-ray study and those calculated by substituting the $^2J(^1H-^{119}Sn)$ values listed in Table 7 in the Lockhart–Manders equation.[33] By contrast, the conductivity measurements (see the Experimental section) suggest considerable dynamic competition among dmso and the non-pyridoxine ligands (H_2O, NO_3^-, Cl^-) for the other co-ordination positions around Sn.

The low solubility of the complexes in dmso, together with the breadth of some signals (probably due to the interchanges mentioned above), limited the ^{13}C NMR study of the complexes to **1**. The deshielding of C(3), C(4) and C(9) over and above the effect of N-protonation, and the closeness of these signals to their positions in the solid-state spectrum, indicate that the organometal moiety is still chelated by O(2) and O(1).

Proton and ^{13}C NMR data in D_2O for PN, PN·HCl and the complexes are listed in Table 8. Note that in this solvent the H(6) signal is at lower field for PN·HCl than for PN, whereas in dmso the opposite is true.[34] The ^{13}C NMR signals of PN and PN·HCl were assigned on the basis of published data[11,34,35] and $^1H-^{13}C$ HMBC and HMQC spectra (Fig. 8). In the spectrum of PN the C(3) signal lies downfield and the C(6) signal upfield from their positions in the spectrum recorded in dmso; the erroneous assignment of Hartman and Kelusky[35] can perhaps be attributed to this peculiar behaviour. The spectra of PN·HCl in D_2O and dmso also differ in respect of these two carbons. All the ^1H signals in D_2O differ little from one complex to another and their chemical shifts are in all cases between those of PN and PN·HCl, showing that in this solvent the compounds are fundamentally dissociated and that the mono- and di-deprotonated species do not remain as such in solution. The ^{13}C NMR data, which are practically the same for all three complexes, confirm this.

Acknowledgements

We thank Dr. Steuenagel of Bruker Spectrospin for high-speed ^{13}C NMR solid-state spectra, and the Xunta de Galicia, Spain, for financial support under Project XUGA 20316 B94. F. C. thanks the Instituto de Cooperación Iberoamericana, Spain, for a grant.

References

1 T. M. Tsangaris and D. R. Williams, *Appl. Organomet. Chem.*, 1992, **6**, 3.
2 M. M. McGrady and R. S. Tobias, *Inorg. Chem.*, 1964, **3**, 1157; G. Arena, R. Purrello, E. Rizzarelli, A. Gianguzza and L. Pellerito, *J. Chem. Soc., Dalton Trans.*, 1989, 773; R. Barbieri and A. Silvestri, *Inorg. Chim. Acta*, 1991, **188**, 95; T. Natsume, S. Aizawa, K. Hatano and S. Funahashi, *J. Chem. Soc., Dalton Trans.*, 1994, 2749.
3 G. Arena, A. Gianguzza, L. Pellerito, S. Musumeci, R. Purrello and E. Rizzarelli, *J. Chem. Soc., Dalton Trans.*, 1990, 2603; G. Arena, A. Contino, S. Musumeci and R. Purrello, *J. Chem. Soc., Dalton Trans.*, 1990, 3383; G. Arena, R. Cali, A. Contino, A. Musumeci, S. Musumeci and R. Purrello, *Inorg. Chim. Acta*, 1995, **237**, 187; N. Buzás, T. Gajda, E. Kuzmann, L. Nagg, A. Vértes and K. Burger,

Main Group Met. Chem., 1995, **18**, 641; M. M. Shokvy, *Talanta*, 1996, **43**, 177.
4 C. De Stefano, C. Foti, A. Gianguzza, M. Martino, L. Pellerito and S. Sammartano, *J. Chem. Eng. Data*, 1996, **41**, 511.
5 (*a*) J. S. Casas, M. V. Castaño, M. S. García-Tasende, T. Perez Alvarez, A. Sánchez and J. Sordo, *J. Inorg. Biochem.*, 1996, **61**, 97; (*b*) J. S. Casas, A. Castiñeiras, María D. Couce, G. Martinez, J. Sordo and J. M. Varela, *J. Organomet. Chem.*, 1996, **517**, 165.
6 I. Haiduc and C. Silvestri, in *Organometallics in Cancer Chemotherapy*, CRC Press, Boca Raton, FL, 1989, vol. 1, p. 129; M. T. Musmeci, G. Madonia, M. T. Lo Giudice, A. Silvestri, G. Ruisi and R. Barbieri, *Appl. Organomet. Chem*., 1992, **6**, 127; K. Burger, L. Nagy, N. Buzás, A. Vértes and H. Mehner, *J. Chem. Soc*., *Dalton Trans*., 1993, 2499.
7 E. E. Snell, in *Vitamin B_6 Pyridoxal Phosphate*, eds. D. Dolphin, R. Poulson and O. Avramovic, J. Wiley, New York, 1986, Part A, ch. 1, p. 6.
8 (*a*) S. P. Sudhakara Rao, K. I. Varughese and H. Manohar, *Inorg. Chem.*, 1986, **25**, 734; (*b*) I. I. Mathews and H. Manohar, *J. Chem. Soc*., *Dalton Trans*, 1991, 2139; (*c*) I. I. Mathews, S. P. Sudhakara Rao and M. Nethaji, *Polyhedron*, 1992, **11**, 1397.
9 (*a*) J. H. K. A. Acquaye and M. F. Richardson, *Inorg. Chim. Acta*, 1992, **201**, 101; (*b*) V. Kh. Sabirov, M. A. Porai-Koshitz and Yu T. Struchkov, *Acta Crystallogr.*, *Sect. C*, 1993, **49**, 1611 and refs. therein.
10 K. Yang, L. Wang, J. Wu and F. Dong, *J. Inorg. Biochem.*, 1993, **52**, 145.
11 (*a*) A. Mosset, F. Nepven-Juras, R. Haran and J. J. Bonnet, *J. Inorg. Nucl. Chem.*, 1978, **40**, 1259; (*b*) M. D. Couce, J. M. Varela, A. Sánchez, J. S. Casas, J. Sordo and M. López-Rivadulla, *J. Inorg. Biochem.*, 1992, **46**, 17.
12 (*a*) M. Gielen, R. Willem, T. Mancilla, J. Ramharter and E. Joosen, *Silicon*, *Germanium*, *Tin*, *Lead Compd*., 1986, **9**, 349; (*b*) F. Kayser, M. Biesemans, M. Gielen and R. Willem, *Main Group Met. Chem.*, 1994, **17**, 559; (*c*) F. Kayser, M. Biesemans, M. Gielen and R. Willem, *Magn. Reson. Chem.*, 1994, **32**, 358.
13 N. Walker and D. Stuart, *Acta Crystallogr.*, *Sect. A*, 1983, **39**, 158.
14 G. M. Sheldrick, SHELX 76, Program for crystal structure determination, University of Cambridge, 1976.
15 C. K. Johnson, ORTEP, Report ORNL-3794, Oak Ridge National Laboratory, Oak Ridge, TN, 1965.
16 E. Keller, SCHAKAL, A program for plotting molecular and crystal structures, University of Freiburg, 1988.
17 D. T. Cromer and J. B. Mann, *Acta Crystallogr*., *Sect. A*, 1968, **24**, 321.
18 D. T. Cromer and D. Liberman, *J. Chem. Phys.*, 1970, **53**, 1891.
19 R. F. Stewart, E. R. Davidson and W. T. Simpson, *J. Chem. Phys.*, 1965, **42**, 3175.
20 M. Webster and P. H. Collins, *Inorg. Chim. Acta*, 1974, **9**, 157.
21 H. Reuter and D. Schröder, *Acta Crystallogr.*, *Sect. C*, 1992, **48**, 1112.
22 T. Natsume, S. Aizawa, K. Hatamo and S. Funahashi, *J. Chem. Soc*., *Dalton Trans*., 1994, 2749 and refs. therein.
23 A. Sánchez González, A. Castiñeiras, J. S. Casas, J. Sordo and U. Russo, *Inorg. Chim. Acta*, 1994, **216**, 257 and refs. therein.
24 B. Salgado, E. Freijanes, A. Sánchez González, J. S. Casas, J. Sordo, U. Casellato and R. Graziani, *Inorg. Chim. Acta*, 1991, **185**, 137.
25 J. E. Huheey, E. A. Keiter and R. L. Keiter, *Inorganic Chemistry: Principles of Structure and Reactivity*, Harper Collins College Publishers, New York, 4th edn., 1993, p. 292.
26 A. R. Forrester, S. J. Garden, R. Alan Howie and J. L. Wardell, *J. Chem. Soc*., *Dalton Trans*., 1992, 2615 and refs. therein.
27 J. Longo, K. J. Franklin and M. F. Richardson, *Acta Crystallogr*., *Sect. B*, 1982, **38**, 2721.
28 G. E. Bacon and J. S. Plant, *Acta Crystallogr.*, *Sect. B*, 1980, **36**, 1130.
29 W. Kabsch, *Acta Crystallogr.*, *Sect. A*, 1976, **32**, 922.
30 T. A. Franklin and M. F. Richardson, *Inorg. Chim. Acta*, 1980, **46**, 191.
31 N. A. Drobinskaya, L. V. Inova, M. Ya. Karpeiskii and V. L. Florent'ev, *Chem. Heterocycl. Compd.* (*Engl. Transl.*), 1973, **7**, 330.
32 J. S. Casas, E. E. Castellano, M. D. Couce, A. Sánchez, J. Sordo, J. M. Varela and J. Zukerman-Schpector, *Inorg. Chem.*, 1995, **34**, 2430.
33 T. P. Lockhart and W. F. Manders, *Inorg. Chem.*, 1986, **25**, 892.
34 R. Haran, F. Nepveu-Juras and J.-P. Laurent, *Org. Magn. Reson.*, 1977, **10**, 203.
35 J. S. Hartman and E. C. Kelusky, *Can. J. Chem*., 1979, **57**, 2118.

Received 8*th May* 1997; *Paper* 7/03167J